

MAGNETORESISTANCE AND MAGNETOCAPACITANCE
IN A TWO-DIMENSIONAL ELECTRON GAS
IN THE PRESENCE OF A ONE-DIMENSIONAL SUPERLATTICE POTENTIAL

Dieter Weiss

Max-Planck-Institut für Festkörperforschung, Heisenbergstraße 1
D-7000 Stuttgart 80, Federal Republic of Germany

A novel type of magnetoresistance oscillation is observed in a two-dimensional electron gas in a high mobility GaAs-AlGaAs heterostructure with a holographically induced lateral periodic modulation in one direction. The modulation arises due to the persistent photoconductivity of the samples at low temperatures. The experiments show that the $1/B$ periodicity of the additional oscillations is determined by the carrier density N_s and the period a of the grating, reflecting the commensurability of cyclotron diameter and modulation period. The key to the explanation of the novel magnetotransport oscillations is an oscillatory linewidth of the modulation broadened Landau bands. To demonstrate this we have performed magnetocapacitance measurements in order to obtain direct information about the density of states of the modulated two-dimensional electron gas

INTRODUCTION

At low temperatures the magnetoresistance of a degenerate two-dimensional electron gas (2-DEG) exhibits the well known Shubnikov-de Haas (SdH) oscillations reflecting the discrete nature of the degenerate Landau energy spectrum [1]. A superimposed one-dimensional periodic potential lifts the degeneracy of the Landau levels and leads to a novel type of magnetoresistance oscillation periodic in $1/B$ as long as the period of the modulation is small compared to the mean free path of the electrons [2]. The periodicity of these oscillations is governed by an interesting commensurability problem owing to the presence of two length scales, the period a of the potential and the cyclotron radius R_C at the Fermi energy [2,3]. In selectively doped AlGaAs-GaAs heterostructures a persistent increase in the two-dimensional electron density is observed at temperatures below $T=150\text{K}$ if the device is illuminated with infrared or visible light. This phenomenon is usually explained on the basis of the properties of DX-centers which seem to be related to a deep Si donor. The increase in the electron density depends on the photon flux absorbed in the semiconductor so that a spatially modulated photon flux generates a modulation in the carrier density. In our measurements a holographic illumination of the heterostructure at liquid helium temperatures is used to produce a periodic potential

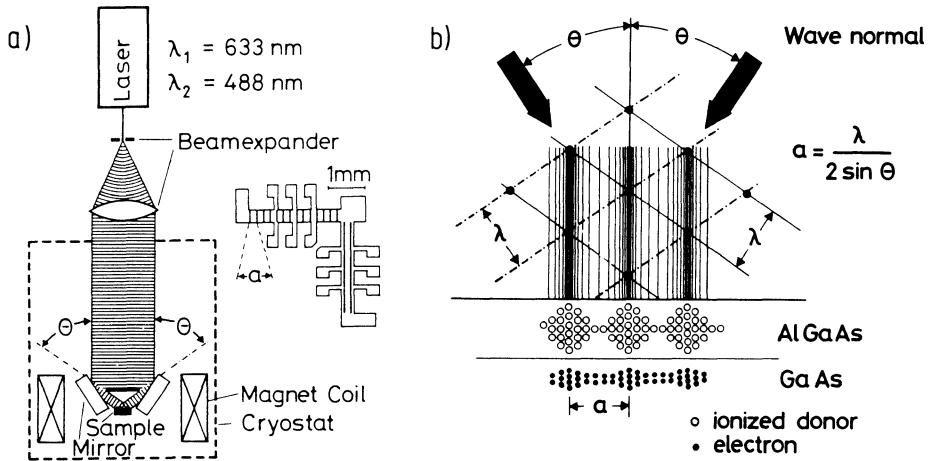


Figure 1. Schematic experimental set up and top view of the L shaped sample geometry with sketched interference pattern (a). Principle of holographic illumination by spatial modulation of the concentration of ionized donors in the AlGaAs layer and of electrons in the 2-DEG using two interfering laser beams (b). The interference pattern is shown schematically – the period a is determined by the wavelength λ and the angle Θ

with a period on the order of the wavelength of the interfering beams, a method first used by Tsubaki et al. [4]. The potential modulation obtained by this technique is on the order of 1 meV where the Fermi energy E_F in our samples is typically 10 meV.

In the first part of this contribution the experiment displaying the novel magnetoresistance oscillations is briefly reviewed followed by a brief discussion of the Landau energy spectrum in the presence of a superimposed one-dimensional potential and a sketch of the theory explaining the observed oscillatory magnetoresistance. In the last section the modification of the energy spectrum is experimentally demonstrated by magnetocapacitance measurements reflecting directly the thermodynamic density of states (DOS) at the Fermi energy.

MAGNETORESISTANCE OSCILLATIONS

The experiments were carried out using conventional AlGaAs-GaAs heterostructures grown by molecular beam epitaxy with carrier densities between $1.5 \cdot 10^{11} \text{ cm}^{-2}$ and $4.3 \cdot 10^{11} \text{ cm}^{-2}$ and low temperature mobilities ranging from $0.23 \cdot 10^6 \text{ cm}^2/\text{Vs}$ to $1 \cdot 10^6 \text{ cm}^2/\text{Vs}$. Illumination of the samples increases both the carrier density and the mobility at low temperatures. We have chosen an L-shaped geometry (sketched on the right hand side of Fig.1a) to investigate the magnetotransport properties parallel and perpendicular to the interference fringes. Some of the samples investigated have an evaporated semi-transparent NiCr front gate (thickness $\approx 8 \text{ nm}$) in order to vary the carrier density as well as to carry out magnetocapacitance measurements after holographic illumination. A sketch of the experiment exploiting the persistent photoconductivity to periodically modulate the positive background charge in the AlGaAs-layer is shown in Fig.1a and 1b. We used either a 5mW HeNe laser ($\lambda = 633 \text{ nm}$) or a 3mW Argon-Ion laser ($\lambda = 488 \text{ nm}$) mounted on top of the sampleholder. The expanded laser beam entered the sampleholder through a quartz window and a shutter ensuring typical illumination times of about 100

ms. Two mirrors mounted close to the sample were used to create two interfering plane waves. The advantage of this kind of ‘microstructure engineering’ is its simplicity and the achieved high mobility of the microstructured sample due to the absence of defects introduced by the usual pattern transfer techniques [5].

The result of standard magnetoresistance measurements carried out perpendicular (ρ_{\perp}) and parallel (ρ_{\parallel}) to the periodic modulation is shown in Fig.2. In addition to the usual Shubnikov-de Haas oscillations appearing at about 0.5T additional oscillations

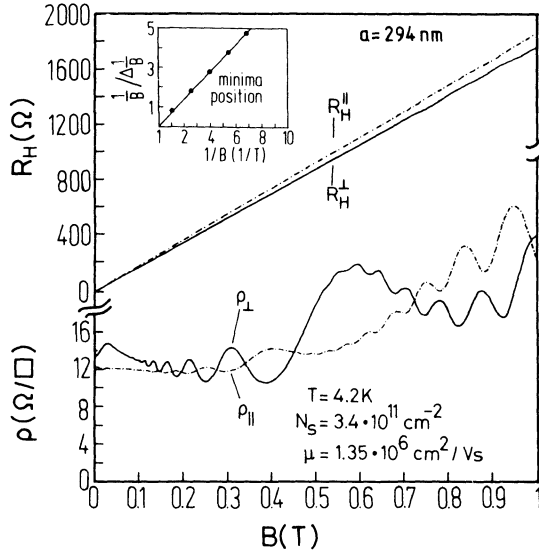


Figure 2. Magnetoresistivity ρ and Hall resistance R_H parallel and perpendicular to the interference fringes. The positions of the minima of ρ_{\perp} are plotted in the inset demonstrating the $1/B$ periodicity of the novel oscillations

become visible at even lower magnetic fields. While pronounced oscillations of this new type dominate ρ_{\perp} at low magnetic fields, weaker oscillations with a phase shift of 180° relative to the ρ_{\perp} data are visible in the ρ_{\parallel} measurements. No additional structure appears in the Hall resistance. The novel oscillations are, analogous to SdH oscillations, periodic in $1/B$ as is displayed in the inset of Fig.2. As the temperature is increased from 2.2K to 4.2K the SdH oscillations are strongly damped whereas the additional oscillations are apparently unaffected. The periodicity is obtained from the minima of ρ_{\perp} , which can be characterized by the commensurability condition

$$2R_c = \left(\lambda - \frac{1}{4}\right)a, \quad \lambda = 1, 2, 3, \dots, \quad (1)$$

between the cyclotron diameter at the Fermi level, $2R_c = 2v_F/\omega_c = 2l^2k_F$, and the period a of the modulation. Here $k_F = \sqrt{2\pi N_s}$ is the Fermi wavenumber, $l = \sqrt{\hbar/eB}$ the magnetic length, and $\omega_c = \hbar/ml^2$ the cyclotron frequency with the effective mass $m = 0.067m_0$ of GaAs. For magnetic field values satisfying Eq.(1) minima are observed in ρ_{\perp} . The periodicity $\Delta(1/B)$ can easily be deduced from Eq.(1)

$$\Delta \frac{1}{B} = e \frac{a}{2\hbar k_F} \quad (2)$$

The validity of Eq.(1) has been confirmed by performing these experiments on different samples, by changing the carrier density with an applied gate voltage, and by using two laser wavelengths in order to vary the period a [2]. This is demonstrated in Fig.3 where the periodicity $\Delta(1/B)$ (displayed as carrier density $n = \frac{e}{\pi h}(\Delta \frac{1}{B})^{-1}$) is plotted as a function of the carrier density N_s and the period a . The solid lines correspond to Eq.(2). Recently similar magnetoresistance oscillations have also been observed in conventionally microstructured samples by Winkler et al. [6].

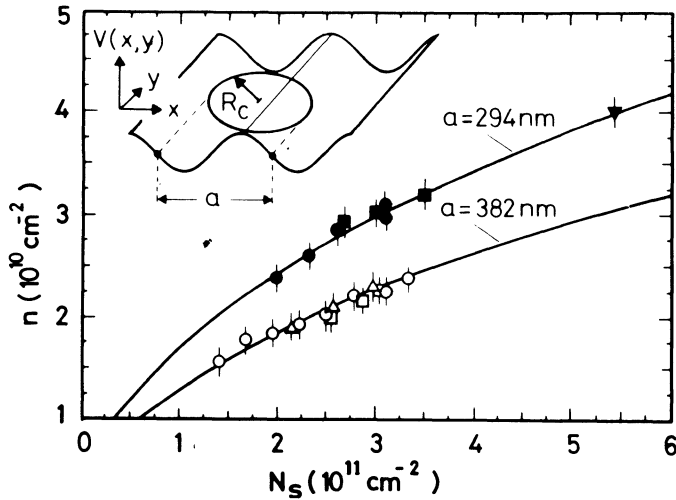


Figure 3. $n = \frac{e}{\pi h}(\Delta \frac{1}{B})^{-1}$ versus N_s . Full symbols correspond to a laser wavelength $\lambda=488\text{nm}$, open symbols to $\lambda=633\text{nm}$ and different symbols represent different samples. The solid lines are calculated using the condition that the cyclotron orbit diameter $2R_c$ is equal to an integer multiple of the interference period a , as is sketched in the inset

SKETCH OF THE THEORY

Since the theory of these novel type of oscillation is discussed in detail by Gerhardtts in this volume I restrict myself to a rough sketch of it. A periodic potential, e.g., in x direction $V(x) = V_0 \cos(Kx)$ with $K = 2\pi/a$ lifts the degeneracy of the Landau levels, and yields eigenstates $|x_0 n\rangle$ which carry current in the y -direction,

$$\langle x_0 n | v_y | x_0 n \rangle = -\frac{1}{m\omega_c} \frac{d\varepsilon_n}{dx_0} = \frac{1}{\hbar} \frac{d\varepsilon_n}{dk_y}, \quad (3)$$

where x_0 is the center coordinate $x_0 = -l^2 k_y$ and n is the Landau level (LL) index. On the other hand $\langle x_0 n | v_x | x_0 n \rangle = 0$, which is the origin of the anisotropic transport coefficients observed. The width of the Landau bands oscillates, which is most easily understood within first order perturbation theory with respect to V_0 . This yields for the energy spectrum plotted in Fig.4

$$\varepsilon_n^{(1)}(x_0) = \hbar\omega_c(n + \frac{1}{2}) + V_0 \cos(Kx_0) e^{-\frac{1}{2}X} L_n(X), \quad (4)$$

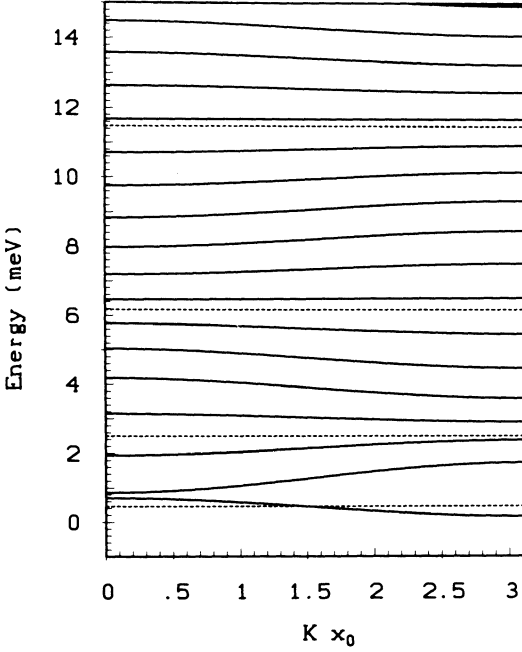


Figure 4. Calculated energy bands $\epsilon_n^1(x_0)$ for $B=0.5T$, $V_0 = 1meV$, $a = 100nm$ and material parameters of GaAs. The dotted lines correspond to energies of zero band width

where $X = \frac{1}{2}K^2l^2$, and exhibits qualitatively the same features as the exact energy spectrum [3]. For fixed magnetic field (fixed X), the Laguerre polynomial $L_n(X)$ oscillates as a function of its index n [7]. The flat band condition, $L_n(X) = 0$, can be expressed in terms of the cyclotron radius $R_C = l\sqrt{2n+1}$, and is identical with Eq.1 [3]. The flat band energies are indicated for $\lambda = 1, \dots, 4$ as dotted lines in Fig.4. In a real physical system the flat bands are of course collision broadened and described by a linewidth Γ . The origin of the oscillations is that the wavefunctions, having a spatial extent of approximately $2R_C$, sense effectively the average value of the periodic potential over an interval of length $2R_C$. The nonvanishing matrix elements $\langle x_{on}|v_y|x_{on}\rangle$ lead to an additional contribution to the conductivity σ_{yy} which becomes important for high-mobility systems [3]. It is this contribution of current carrying states at the Fermi level, which has no counterpart in σ_{xx} , which accounts for the anisotropy of the transport coefficients and leads to oscillations with minima if flat bands occur at the Fermi energy. Since σ_{yx} shows no noticeable oscillations and since $\sigma_{yx}^2 \gg \sigma_{xx}\sigma_{yy}$, one has $\rho_{xx} \approx \sigma_{yy}/\sigma_{yx}^2$, $\rho_{yy} \approx \sigma_{xx}/\sigma_{yx}^2$, and the minima of σ_{yy} coincide with those of ρ_{xx} . The result of a calculation carried out in the Kubo formalism is shown in Fig.5 where the calculated $\rho_{xx} = \rho_{\perp}$ and $\rho_{yy} = \rho_{\parallel}$ curves are compared to experimental ones. In this experiment a higher modulation amplitude has been achieved than in previously published data taken from the same sample material [3]. The resulting higher amplitudes of the novel oscillations are therefore well described using a modulation amplitude $V_0 = 0.6meV$ in the calculations which is twice as large as in Ref. [3]. Details of the calculation are discussed by Gerhardtts in this volume. The novel oscillations of ρ_{\perp} are nicely reproduced by the calculation, which for ρ_{\parallel} essentially yields the Drude result (independent of B). The temperature dependence of the novel oscillations is much weaker than that of the SdH oscillations, since the relevant energy is the distance between flat bands, which is much larger than the mean distance between adjacent bands. A similar model, based on the Boltzmann transport theory, has been used

by Winkler et al. [6] to explain the additional oscillations. A semiclassical picture explaining the effect as a resonance between the periodic cyclotron orbit motion and the oscillating $\vec{E} \times \vec{B}$ drift of the orbit center induced by the potential grating has been suggested by Beenakker [8]. Such a semiclassical approximation, however, does not describe the whole physics of the observed phenomena as will be shown in the next section.

MAGNETOCAPACITANCE EXPERIMENTS

The oscillations of the LL linewidth, mentioned above, should in turn lead to oscillations of the density of states. Since for fixed magnetic field, the number of states per Landau band is fixed, oscillations of the band width should lead to oscillations of the

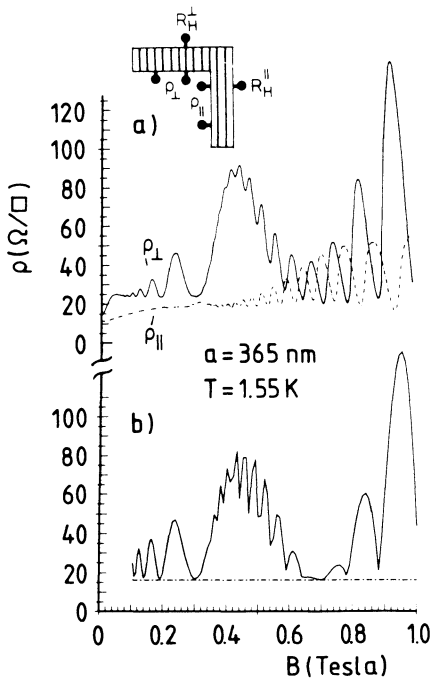


Figure 5. Magnetoresistivities for current perpendicular (ρ_{\perp} , solid lines) and parallel (ρ_{\parallel} , dash dotted lines) to the interference fringes, as indicated in the inset, for a sample with $N_S = 3.39 \cdot 10^{11} \text{ cm}^{-2}$, $\mu = 1.1 \cdot 10^6 \text{ cm}^2/\text{Vs}$, and $a = 365 \text{ nm}$, (a) measured and (b) calculated for temperature $T=1.55 \text{ K}$, using $V_0=0.6 \text{ meV}$. Calculation after Gerhardt's Ref.[3]

peak density of states with maxima for flat bands satisfying Eq.(1). This behaviour is demonstrated experimentally in magnetocapacitance measurements. The capacitance between the semi-transparent gate and the 2-DEG is measured by applying an ac-voltage between the gate and one channel contact and measuring the out-of-phase ac-current with lock-in techniques. The oscillations of the capacitance as a function of the magnetic field are directly connected to the DOS at the Fermi energy [9,10,11,13]. In a homogeneous 2-DEG it has been shown experimentally that the LL linewidth (due to collision broadening) Γ has a magnetic field dependence of the form $\Gamma \propto B^{\alpha}$ with

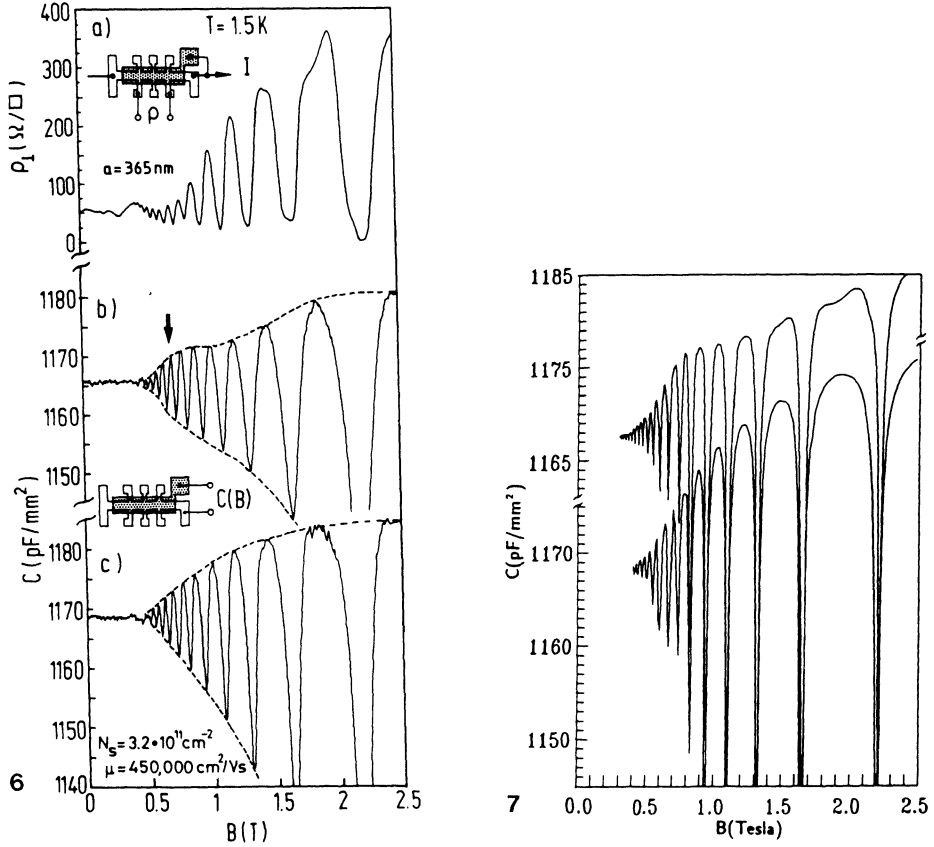


Figure 6. Measured magnetoresistivity ρ_{\perp} (a) and magnetocapacitance (b) of a modulated sample compared to the capacitance of an essentially unmodulated sample (c). The arrow corresponds to the magnetic field value fulfilling Eq.1 for $\lambda = 1$. The insets sketch the measurements

Figure 7. Calculated magnetocapacitance versus magnetic field for $N_S = 3.2 \cdot 10^{11} \text{ cm}^{-2}$ and $a = 365 \text{ nm}$. A B-independent linewidth is chosen to be $\Gamma = 0.3 \text{ meV}$. The upper curve is for $V_0 = 0.7 \text{ meV}$, and the lower one for the weak modulation $V_0 = 0.1 \text{ meV}$. After Zhang Ref.[16]

$0 \leq \alpha \leq 0.5$ [12,13], whereas theoretically $\Gamma \propto \sqrt{B}$ is expected for short range scatterers and a B-independent Γ for long range scatterers [14,15]. Since the Landau degeneracy is proportional to B, the peak values of the DOS in the individual LL's and, as a consequence, the peak values of the capacitance, are expected to increase monotonically, with a structureless envelope, with increasing magnetic field. On the other hand the envelope of the magnetocapacitance minima decreases monotonically with B due to the increasing LL separation $\hbar\omega_c$. In Fig.6 the magnetocapacitance data after an initial holographic illumination (90ms long) (b) is compared with the capacitance measured after an additional illumination which essentially smears out the periodic modulation (c). In Fig.6a the magnetoresistivity ρ_{\perp} measured under the same experimental conditions as the magnetocapacitance data in Fig.6b is shown. The carrier density in Fig.6c has been adjusted to the same value as before the additional illumination using a negative gate voltage. In contrast to Fig.6c, where the magnetocapacitance behaves as one usually observes in a 2-DEG, the capacitance oscillations in Fig.6b display a pronounced modulation of both the minima and maxima which is easily explained from the energy spectrum plotted in Fig.4. At about 0.69T (marked by an arrow) where the cyclotron diameter at the Fermi level equals three quarters of the period a , ρ_{\perp} in Fig.6a displays the last minimum ($\lambda = 1$) corresponding to the last flat band condition. Therefore the magnetocapacitance values near 0.69T are approximately equal in Fig.6b and Fig.6c. If now the magnetic field is increased, broader Landau bands are swept through the Fermi level, and cause the nonmonotonic behaviour visible in Fig.6b. At higher magnetic fields the level broadening saturates and the usual LL degeneracy again raises the DOS in a LL with increasing field. It should be mentioned that the modulation effect is observed for different angles between the one-dimensional modulation and the long axis of the Hall bar as is expected for a thermodynamic quantity in contrast, of course, to the magnetoresistivity. In order to check the magnetocapacitance data theoretically microscopic calculations of the density of states based on a generalisation of the well known selfconsistent Born approximation have been performed by Zhang [16]. Parts of this theory are also discussed by Gerhardtts (this volume) and therefore I only present the results obtained from such calculations. In Fig.7 calculated magnetocapacitance data for a modulated (upper curve) and an essentially unmodulated 2-DEG are shown which are in good agreement with the experimental data. The collision broadening used in the calculations was $\Gamma = 0.3\text{meV}$ in agreement with previous magnetocapacitance measurements carried out on homogeneous samples with similar mobility [13].

I am indebted to K. v.Klitzing and R.R. Gerhardtts for many discussions and comments, D. Heitmann for helpful suggestions and C. Zhang for performing numerical calculations. I also want to thank K. Ploog and G. Weimann for providing me with high quality samples, and S. Bending for a critical reading of the manuscript. The work was supported in part by the Bundesministerium für Forschung und Technologie, West Germany.

REFERENCES

- [1] L. Shubnikov, W. J. de Haas, *Leiden Commun.* **207a**, **207c**, **207d**, **210a** (1930)
- [2] D. Weiss, K. v. Klitzing, K. Ploog, G. Weimann *Europhys. Lett.* **8**, 179 (1989); also in *The Application of High Magnetic Fields in Semiconductor Physics*, ed. G. Landwehr, Springer Series in Solid-State Sciences (Berlin), to be published
- [3] R. R. Gerhardtts, D. Weiss, K. v. Klitzing; *Phys. Rev. Lett.* **62**, 1173 (1989)

- [4] K. Tsubaki, H. Sakaki, J. Yoshino, Y. Sekiguchi, *Appl. Phys. Lett.* **45**, 663 (1984)
- [5] For recent work in this field see *Physics and Technology of Submicron Structures*, Vol. 83 of Springer Series Solid-State Sciences, ed. by H. Heinrich, G. Bauer, and F. Kuchar (Springer, Berlin, 1988)
- [6] R. W. Winkler, J. P. Kotthaus, K. Ploog; *Phys. Rev. Lett.* **62**, 1177 (1989)
- [7] M. Abramowitz and I. A. Stegun, ed., *Handbook of Mathematical Functions*, (Dover Publications, New York (1972))
- [8] C.W.J. Beenakker, preprint
- [9] T. P. Smith, B. B. Goldberg, P. J. Stiles, M. Heiblum, *Phys. Rev.* **B32**, 2696 (1985)
- [10] V. Mosser, D. Weiss, K. v. Klitzing, K. Ploog, G. Weimann, *Solid State Commun.* **58**, 5 (1986)
- [11] V. Gudmundsson, R. R. Gerhardt, *Phys. Rev.* **B35**, 8005 (1987)
- [12] see e.g.: E. Gornik, R. Lassnig, G. Strasser, H. L. Störmer, A. C. Gossard, W. Wiegmann, *Phys. Rev. Lett.* **54**, 1820 (1985); J. P. Eisenstein, H. L. Störmer, V. Narayanamurti, A. Y. Cho, A. C. Gossard, *Phys. Rev. Lett.* **55**, 1820 (1985) 539 (1985)
- [13] D. Weiss, K. v. Klitzing in *High Magnetic Fields in Semiconductor Physics*, ed. G. Landwehr, Springer Series in Solid-State Sciences **71**, (Berlin), 1987
- [14] T. Ando, Y. Uemura, *J. Phys. Soc. Jpn.* **36**, 959 (1974)
- [15] R. R. Gerhardt, *Z. Physik* **B21**, 285 (1975)
- [16] D. Weiss, C. Zhang, R.R. Gerhardt, K. v. Klitzing, G. Weimann, submitted to *Phys. Rev. B*